Femtosecond versus picosecond laser machining of nano-gratings and micro-channels in silica glass

Costantino Corbari,[1,*] Audrey Champion,[2] Mindaugas Gecevičius,[1] Martynas Beresna,[1] Yves Bellouard,[2] and Peter G. Kazansky [1]

[1]*Optoelectronics Research Centre, University of Southampton, SO17 1BJ, United Kingdom*
[2]*Mechanical Engineering Dept. Eindhoven University of Technology, Eindhoven, The Netherlands*
**coc@orc.soton.ac.uk*

Abstract: The ability of 8 picosecond pulse lasers for three dimensional direct-writing in the bulk of transparent dielectrics is assessed through a comparative study with a femtosecond laser delivering 600 fs pulses. The comparison addresses two main applications: the fabrication of birefringent optical elements and two-step machining by laser exposure and post-processing by chemical etching. Formation of self-organized nano-gratings in glass by ps-pulses is demonstrated. Differential etching between ps-laser exposed regions and unexposed silica is observed. Despite attaining values of retardance (>100 nm) and etching rate (2 μm/min) similar to fs pulses, ps pulses are found unsuitable for bulk machining in silica glass primarily due to the build-up of a stress field causing scattering, cracks and non-homogeneous etching. Additionally, we show that the so-called "quill-effect", that is the dependence of the laser damage from the direction of writing, occurs also for ps-pulse laser machining. Finally, an opposite dependence of the retardance from the intra-pulse distance is observed for fs- and ps-laser direct writing.

OCIS codes: (140.3390) Laser materials processing; (140.7090) Ultrafast lasers; (160.6030) Silica.

References and links

1. S. S. Mao, F. Quere, S. Guizard, X. Mao, R. E. Russo, G. Petite, and P. Martin, ""Dynamics of femtosecond laser interactions with dielectrics," Appl. Phys **79**, 1695–1709 (2004).
2. C. B. Schaffer, A. Brodeur, and E. Mazur, "Laser-induced breakdown and damage in bulk transparent materials induced by tightly focused femtosecond laser pulses," Meas. Sci. Technol. **12**(11), 1784–1794 (2001).
3. B. C. Stuart, M. D. Feit, S. Herman, A. M. Rubenchik, B. W. Shore, and M. D. Perry, "Nanosecond-to-femtosecond laser-induced breakdown in dielectrics," Phys. Rev. B Condens. Matter **53**(4), 1749–1761 (1996).
4. I. M. Burakov, N. M. Bulgakova, R. Stoian, A. Mermillod-Blondin, E. Audouard, A. Rosenfeld, A. Husakou, and I. V. Hertel, "Spatial distribution of refractive index variations induced in bulk fused silica by single ultrashort and short laser pulses," J. Appl. Phys. **101**(4), 043506 (2007).
5. S. Juodkazis, H. Misawa, and I. Maksimov, "Thermal accumulation effect in three-dimensional recording by picosecond pulses," Appl. Phys. Lett. **85**(22), 5239–5241 (2004).
6. H. Zhang, S. M. Eaton, and P. R. Herman, "Low-loss Type II waveguide writing in fused silica with single picosecond laser pulses," Opt. Express **14**(11), 4826–4834 (2006), http://www.opticsinfobase.org/oe/abstract.cfm?URI=oe-14-11-4826.
7. B. McMillen, B. T. Zhang, K. P. Chen, A. Benayas, and D. Jaque, "Ultrafast laser fabrication of low-loss waveguides in chalcogenide glass with 0.65 dB/cm loss," Opt. Lett. **37**(9), 1418–1420 (2012).
8. A. Marcinkevičius, S. Juodkazis, M. Watanabe, M. Miwa, S. Matsuo, H. Misawa, and J. Nishii "Femtosecond laser-assisted three-dimensional microfabrication in silica," Opt. Lett. **26**(5), 277–279 (2001).
9. Y. Bellouard, T. Colomb, C. Depeursinge, M. Dugan, A. A. Said, and P. Bado, "Nanoindentation and birefringence measurements on fused silica specimen exposed to low-energy femtosecond pulses," Opt. Express **14**(18), 8360–8366 (2006), http://www.opticsinfobase.org/oe/abstract.cfm?URI=oe-14-18-8360.
10. Y. Shimotsuma, P. G. Kazansky, J. R. Qiu, and K. Hirao, "Self-organized nanogratings in glass irradiated by ultrashort light pulses," Phys. Rev. Lett. **91**(24), 247405 (2003).

#174210 - $15.00 USD Received 13 Aug 2012; revised 27 Sep 2012; accepted 8 Oct 2012; published 11 Feb 2013

11. C. Hnatovsky, R. S. Taylor, E. Simova, V. R. Bhardwaj, D. M. Rayner, and P. B. Corkum, "Polarization-selective etching in femtosecond laser-assisted microfluidic channel fabrication in fused silica," Opt. Lett. **30**(14), 1867–1869 (2005).
12. M. Beresna, M. Gecevicius, and P. G. Kazansky, "Polarization sensitive elements fabricated by femtosecond laser nanostructuring of glass Invited," Opt. Mater. Express **1**(4), 783–795 (2011), http://www.opticsinfobase.org/ome/abstract.cfm?URI=ome-1-4-783.
13. W. Yang, P. G. Kazansky, Y. Shimotsuma, M. Sakakura, K. Miura, and K. Hirao, "Ultrashort-pulse laser calligraphy," Appl. Phys. Lett. **93**(17), 171109 (2008).
14. A. Couairon and A. Mysyrowicz, "Femtosecond filamentation in transparent media," Phys. Rep. **441**(2-4), 47–189 (2007).
15. A. Couairon and L. Berge, "Modeling the filamentation of ultra-short pulses in ionizing media," Phys. Plasmas **7**(1), 193–209 (2000).
16. A. Couairon and P. G. Kazansky, (Personal Communication 2010).
17. W. J. Yang, E. Bricchi, P. G. Kazansky, J. Bovatsek, and A. Y. Arai, "Self-assembled periodic sub-wavelength structures by femtosecond laser direct writing," Opt. Express **14**(21), 10117–10124 (2006), http://www.opticsinfobase.org/oe/abstract.cfm?URI=oe-14-21-10117.
18. S. Richter, M. Heinrich, S. Doring, A. Tunnermann, and S. Nolte, ""Formation of femtosecond laser-induced nanogratings at high repetition rates," Appl. Phys," Adv. Mater. **104**, 503–507 (2011).
19. C. Hnatovsky, R. S. Taylor, P. P. Rajeev, E. Simova, V. R. Bhardwaj, D. M. Rayner, and P. B. Corkum, "Pulse duration dependence of femtosecond-laser-fabricated nanogratings in fused silica," Appl. Phys. Lett. **87**(1), 014104 (2005).
20. A. Champion and Y. Bellouard, "Direct volume variation measurements in fused silica specimens exposed to femtosecond laser," Opt. Mater. Express **2**(6), 789–798 (2012), http://www.opticsinfobase.org/ome/abstract.cfm?URI=ome-2-6-789.
21. J. Canning, M. Lancry, K. Cook, A. Weickman, F. Brisset, and B. Poumellec, "Anatomy of a femtosecond laser processed silica waveguide, Invited," Opt. Mater. Express **1**(5), 998–1008 (2011), http://www.opticsinfobase.org/ome/abstract.cfm?URI=ome-1-5-998.
22. Y. Shimotsuma, M. Sakakura, P. G. Kazansky, M. Beresna, J. R. Qiu, K. Miura, and K. Hirao, "Ultrafast manipulation of self-assembled form birefringence in glass," Adv. Mater. (Deerfield Beach Fla.) **22**(36), 4039–4043 (2010).
23. L. Skuja, K. Kajihara, M. Hirano, and H. Hosono, "Oxygen-excess-related point defects in glassy/amorphous SiO2 and related materials," Nucl. Instrum. Meth. B **286**, 159–168 (2012).
24. Y. M. Cannas, V. Lavinia, and B. Roberto, "Time resolved photoluminescence associated with non-bridging oxygen hole centers in irradiated silica," Nucl. Instrum. Meth. B **266**(12-13), 2945–2948 (2008).
25. S. Richter, F. Jia, M. Heinrich, S. Döring, U. Peschel, A. Tünnermann, and S. Nolte, "The role of self-trapped excitons and defects in the formation of nanogratings in fused silica," Opt. Lett. **37**(4), 482–484 (2012).
26. D. N. Vitek, E. Block, Y. Bellouard, D. E. Adams, S. Backus, D. Kleinfeld, C. G. Durfee, and J. A. Squier, "Spatio-temporally focused femtosecond laser pulses for nonreciprocal writing in optically transparent materials," Opt. Express **18**(24), 24673–24678 (2010), http://www.opticsinfobase.org/oe/abstract.cfm?URI=oe-18-24-24673.
27. Y. Bellouard, E. Barthel, A. A. Said, M. Dugan, and P. Bado, "Scanning thermal microscopy and Raman analysis of bulk fused silica exposed to low-energy femtosecond laser pulses," Opt. Express **16**(24), 19520–19534 (2008), http://www.opticsinfobase.org/oe/abstract.cfm?URI=oe-16-24-19520.
28. S. Rajesh and Y. Bellouard, "Towards fast femtosecond laser micromachining of fused silica: The effect of deposited energy," Opt. Express **18**(20), 21490–21497 (2010), http://www.opticsinfobase.org/oe/abstract.cfm?URI=oe-18-20-21490.
29. C. Hnatovsky, R. S. Taylor, E. Simova, P. P. Rajeev, D. M. Rayner, V. R. Bhardwaj, and P. B. Corkum, ""Fabrication of microchannels in glass using focused femtosecond laser radiation and selective chemical etching," Appl. Phys," Adv. Mater. **84**, 47–61 (2006).

1. Introduction

Material modification by intense laser pulses is intimately related to the dynamics of energy transfer between the laser excited electrons and the lattice [1–3]. Three regimes of material modifications are accessed depending on whether the pulse duration is shorter, comparable or longer than the time required by the hot electrons to transfer their energy to the lattice via electron-phonon scattering. In the following, the discussion is limited to the case of silica glass for which the electron-phonon coupling time is about $\tau_{e^- - ph} \simeq 1\,\mathrm{ps}$ [3].

For a pulse duration $\tau \gg \tau_{e^- - ph}$ electrons and lattice reach thermodynamic equilibrium on the time scale of the pulse duration. Damage, preferentially by phase explosions, occurs when the rate of energy extraction from the focal volume is smaller compared to the energy

#174210 - $15.00 USD Received 13 Aug 2012; revised 27 Sep 2012; accepted 8 Oct 2012; published 11 Feb 2013

deposition rate. For this reason nanosecond pulses are the most suitable for applications requiring material removal such as laser deep drilling and cutting.

Conversely, laser excitation by femtosecond pulses, for which $\tau \ll \tau_{e^- - ph}$, leads to strong non-equilibrium conditions as electrons in the conduction band are heated much faster than they can cool by phonon scattering. The energy is transferred to the lattice after the pulse is passed on a time scale much shorter than the heat diffusion time producing a permanent modification in the material with essentially no collateral damage. In silica glass, the low collateral damage associated with the processing by femtosecond pulses is proving invaluable for optical waveguide inscriptions, for 3D-precision machining and for the realization of birefringent optical elements.

A theoretical framework for pulse durations $\tau \simeq \tau_{e^- - ph}$ is not available due to the intrinsic complexity. It is known, however, that the fluence damage threshold for silica glass departs in the 1-20 ps pulse range from the thermally driven $\sqrt{\tau}$ dependence associated with longer pulses [3]. During single pulse bulk modification of silica glass, Burakov *et al.* showed that long exposure times were correlated to the material expansion leading to a negative refractive index change in the irradiated zones [4]. The generation of pressure waves - resulting in stress accumulation and positive index change in the region surrounding the focal volume - occurs as a consequence of the material expansion.

Despite picosecond lasers are rarely employed for in-bulk processing of wide-bandgap dielectrics, there is a growing body of evidence that this intermediate regime of material modification brings advantages to some specific applications. Juodkazis and Misawa highlighted how thermal induced stress in borosilicate glass irradiated by 12 ps pulses could be exploited for crack-free in-bulk recording [5]. Additionally, investigation of optical waveguides fabricated by laser direct writing with a wide 50-fs to 5-ps range of pulse duration showed the lowest loss of 0.2 dB/cm for 1 ps pulses [6,7]. Stress accumulation and glass densification are also known to accelerate the etching rate of silica, a feature that would be of interest for two-step machining by laser irradiation and chemical etching [8,9]. It has never been investigated whether the formation of self-assembled periodic nanostructures, known as "nanogratings", is possible for these pulse durations [10]. Nanogratings are thought to favor the etchant penetration [11]. They are also associated with form-birefringence that is exploited for the realization of spatially variant phase plates [12].

In this work, we investigate the hypothesis that nanogratings and faster etching rate can be achieved by pulses of duration comparable to the electro-phonon scattering time. The ability of ps-pulses to generate self-assembled nanogratings and to promote selective chemical etching in the laser exposed regions is demonstrated. The suitability of ps-pulses for the fabrication of polarization sensitive elements or for a two-step machining is discussed in terms of retardance, etching rate and morphology of the etched regions by comparison with fs-pulses of the same pulse energy and fluence.

2. Experimental set-up and methods

For laser inscription in the picosecond regime, a mode-locked amplified neodymium-doped yttrium vanadate ($Nd:YVO_4$) laser emitting a train of 8 ps pulses at the wavelength of 1064 nm (Super-Rapid, Lumera Laser GmbH) was employed. In the femtosecond regime laser writing was performed using a mode-locked regenerative amplified Yb:KGW (ytterbium-doped potassium gadolinium tungstate) laser (PHAROS by Light Conversion Ltd.) operating at λ = 1030 nm. The initial laser pulse duration of 300 fs was stretched to 600 fs with the internal pulse stretcher. The pulse duration was monitored with a single-shot autocorrelator. The pulse duration was chosen to match the optimum conditions for the fabrication of spatially variant wave-plates and polarization mode converters [12].

#174210 - $15.00 USD Received 13 Aug 2012; revised 27 Sep 2012; accepted 8 Oct 2012; published 11 Feb 2013

For the experiments, a 25 x 25 x 1 mm^3 silica plate (SPECTROSIL 2000 by UQG ltd.) was used. The laser beam was focused in the bulk of the sample by a 20X aspheric lens with a numerical aperture of 0.5 (New focus 5720).

Two sets of lines were written with both femtosecond and picosecond laser systems using identical parameters except for the pulse duration. The lines were written 100 μm below the surface by translating the sample transversely to the beam propagation direction. In order to prevent changes in the material modifications by reversal of the writing direction, all lines were written in the same direction [13]. Laser inscription was carried out aligning the direction of the light polarization both orthogonal and parallel to the writing direction using a half-wave plate placed immediately before the focusing lens. The writing speed ranged from 25 μm/s to 6400 μm/s and the laser repetition rate was varied from 12.5 kHz to 400 kHz. As the sample is translated, the effective number of pulses, N_{eff}, is given by $N_{eff} = w \times f / v$ with f being the laser repetition rate, v the sample translation speed and w the focal spot diameter. Correspondingly the net fluence or deposited energy is calculated from $F = 4/\pi w^2 \times N_{eff} \times E_p$ where E_p is the pulse energy.

The threshold pulse fluence for multi-shot bulk damage – as inspected by bright light microscopy - in fused silica when focusing the 1064 nm radiation of the ps-laser was experimentally measured as 7.5 ± 0.2 J/cm^2 (E_p = 0.8 μJ, w = 3.68 μm). These parameters were used throughout the work, therefore the same pulse fluence was used in both fs and ps laser inscription experiments.

The threshold for self-focusing for a collimated Gaussian beam is defined by the self-focusing critical power P_{cr} = 4.3 MW [14]. However, when the beam is focused by a lens the occurrence of collapse always requires power above critical (see appendix) [15,16]. Our experimental conditions correspond to optical power P_{in} equal to 1.3 and 0.1 MW for the fs and ps pulses respectively and are therefore well below the threshold for self-focusing.

Nanogratings were characterized by quantitative birefringence measurements (CRi Abrio imaging system). This system allows accurate measurements of the direction of the slow axis of birefringence as well as the strength of the retardance.

After the laser irradiation, the sample was side-lapped and polished to reveal the cross-sections of the laser written lines and remove the layer of glass that could have been affected by surface/edge effect such as beam clipping. Micro-channels were formed by etching the sample with 2.5% hydrofluoric acid (HF) for 80 minutes. The length of the etched channels was measured under bright illumination optical microscopy with a resolution of ± 1 μm.

3. Results and discussion

3.1 Assessment of ps-lasers for the fabrication of spatially-variant phase-plates

In our experiment, exposure of silica glass to picosecond pulses produces a negative refractive index change as checked by digital holographic microscopy. Although it is not a sufficient proof in itself, this negative refractive index change may suggest the presence of nanogratings, so far only observed in laser tracks produced by fs-laser irradiation [10]. Nanogratings are characterized by a succession of nano-layers (~20 nm) separated by apparently unmodified silica with a periodicity in the order of 150-450 nm depending on pulse energy and wavelength [17,18]. The orientation of the nano-planes follows the direction of the laser polarization. Another periodicity, this time along the head-to-tail direction of the laser damage cross-section, may be present with a period of ~λ/n where λ is the laser wavelength and n the refractive index of silica [17,19].

Quantitative birefringence measurements performed on the radial structure shown in Fig. 1(a-c) demonstrates that silica irradiated by picosecond pulses displays both the form-birefringence and the dependence on the orientation of laser polarization expected from nanogratings. The polarization was kept parallel to the writing direction. Figure 1(b) shows that the direction of the slow axis of birefringence, represented by pseudo-colors (see legend

#174210 - $15.00 USD Received 13 Aug 2012; revised 27 Sep 2012; accepted 8 Oct 2012; published 11 Feb 2013

in the top-right corner) is perpendicular to the orientation of the laser polarization. The evidence of

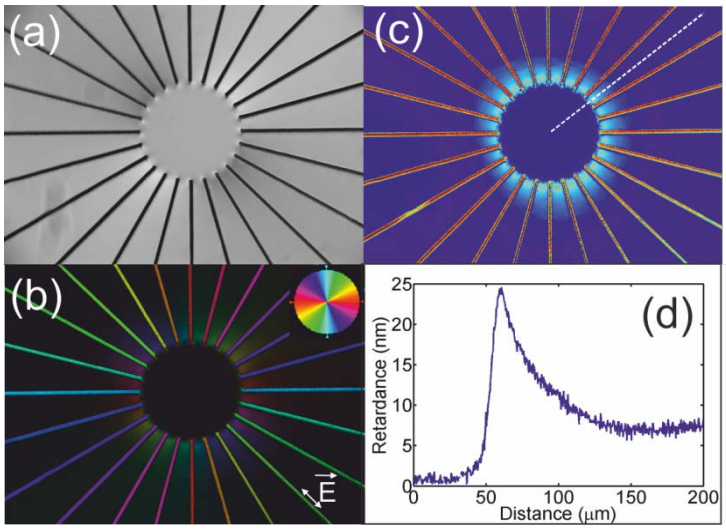

Fig. 1. (a) Optical image of a set of laser tracks radiating out from a virtual circle (∅ = 100 μm). The angle between lines is 15 deg. The Laser polarization is parallel to the writing direction. λ = 1064 nm, NA = 0.65, τ = 8 ps, Ep = 2 μJ, f = 200 kHz, v = 200 μm/s. (b) and (c) Quantitative birefringence measurements of the laser tracks in (a). (b) Pseudo colors represent the angle of the slow axis of birefringence as indicated by the legend in the top right corner. (c) Pseudo colors represent the strength of the retardance. (d) Retardance vs. position along the dashed line in (c). The retardance measured between two laser tracks is indicative of stress-induced birefringence.

nanograting formation with 8 ps pulses was obtained by imaging the cross section of a laser track by Scanning Electron Microscopy (SEM) (Fig. 2). The SEM image shows the top of the cross-section of the laser damage with the nano-planes responsible for the form birefringence aligned perpendicular to the direction of the laser polarization (vertical in Fig. 2). The periodicity is Λ ~250 nm which is comparable to nanogratings formed by fs-laser at similar pulse energies [17]. A second periodicity, Λ ~λ/n ~733 nm, apparently increasing as we move away from the tip of the structure is observed along the horizontal direction. Note that on this SEM image of the cleaved laser track, the irradiated zone seems to protrude out of the plane which is consistent with the volume expansion in the nanogratings zones [4,20,21].

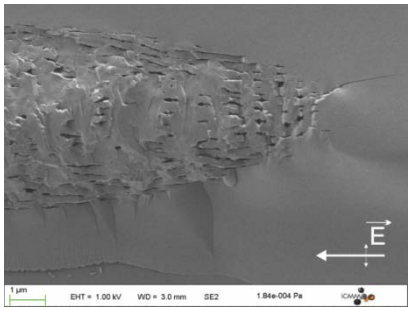

Fig. 2. Field Emission Gun scanning electron microscope (FEG-SEM) image of a cleaved laser track in fused silica. The formation of nano-gratings by ps-pulses is shown. Experimental conditions: λ = 1064 nm, NA = 0.65, τ = 8 ps, E_p = 1 μJ, *f* = 200 kHz, *v* = 200 μm/s. The laser radiation was shining from the right end of the picture. Polarisation oriented perpendicular to the writing direction.

#174210 - $15.00 USD Received 13 Aug 2012; revised 27 Sep 2012; accepted 8 Oct 2012; published 11 Feb 2013

The form-birefringence associated with nanogratings implies that the fabrication of polarization mode converters and spatially variant phase plates is possible even in this long pulse regime [12]. Laser writing by fs and ps pulses was compared by measuring the strength of the retardance. The latter is defined as the product $R \equiv \Delta n \times L$ where Δn is the overall birefringence and L the optical path length. The retardance increases with the net fluence reaching its maximum value at R = 113 ± 10 nm (Fig. 3). The measured value enables writing quarter-wave plates for operation in the visible. Further improvement is possible by using lower NA lens, achieving larger L through the increased Rayleigh range.

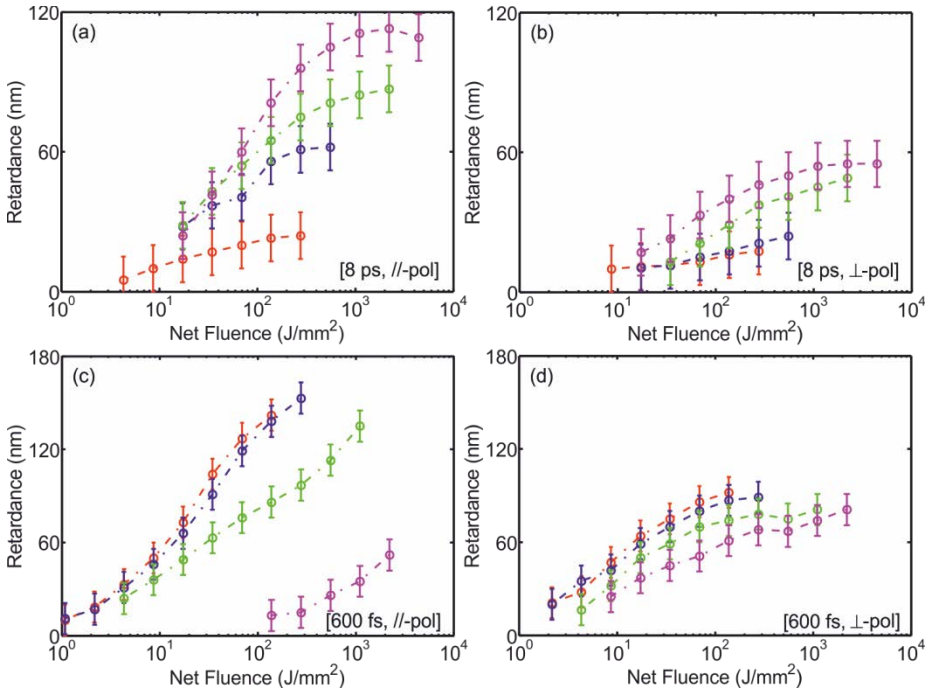

Fig. 3. Measurements of the retardance vs. net laser fluence in tracks processed by (a) 8 ps parallel polarisation and (b) 8 ps transverse polarisation, (c) 600 fs parallel polarisation and (d) 600 fs transverse polarisation. Line colors correspond to: (red) 25 kHz, (blue) 50 kHz, (green), 200 kHz, and (magenta) 400 kHz.

The laser induced retardance presents a marked dependence on the laser repetition rate (Fig. 3). It is an indication that the rate at which the energy is deposited into the glass affects the development of nanogratings. Shimotsuma *et al.* observed a reduction of the laser induced birefringence with increasing repetition rate when irradiating silica glass with 70 fs [22]. Our experiments with 600 fs pulses follow the same trend [Fig. 4(a)]. The drop in the strength of the retardance with reduced intra-pulse distance is interpreted as evidence of the detrimental effect on a microsecond timescale caused by heat accumulation on the formation of nanogratings. In contrast for picosecond pulses the retardance is consistently higher the shorter is the intra-pulse duration [Fig. 4(b)]. We suppose that for long pulses the process of glass modification leading to the formation of nanogratings is facilitated by the presence of defect states with a lifetime comparable to the inter-pulse intervals in our experiments. A plausible candidate is the 2.0 eV absorption (1,9 eV emission) band associated to the excited state of the non-bridging oxygen hole center (NBOHC) that decays with a lifetime of about 10-20 μs [23–25]. The presence of defects creates energy levels within the bandgap of silica and facilitates the production of free electrons that seed the avalanche ionization. It is the strong intensity dependence of the generation of seed electrons by multi-photon ionization that makes damage formation by longer pulses more susceptible to the presence of defects

#174210 - $15.00 USD Received 13 Aug 2012; revised 27 Sep 2012; accepted 8 Oct 2012; published 11 Feb 2013

state. The peak intensity of the 8-ps pulses used in our experiment is 1 TW/cm^2; that is more than 10 times lower than the intensity of the 600 fs pulses (12.5 TW/cm^2) and over 100 times lower than the intensity used by Shimotsuma *et al.*.The estimates on the intensity are given as an upper limit which does not take into account the clamping effect.

It is worth noting here that the process of relaxation of the NBOHC excited state may be responsible for the opposite dependence observed in the fs-regime in place of the temperature effects advocated earlier. For example the much larger number of defects created by fs-pulses may cause stronger absorption of the incoming pulses or defect saturation may occur.

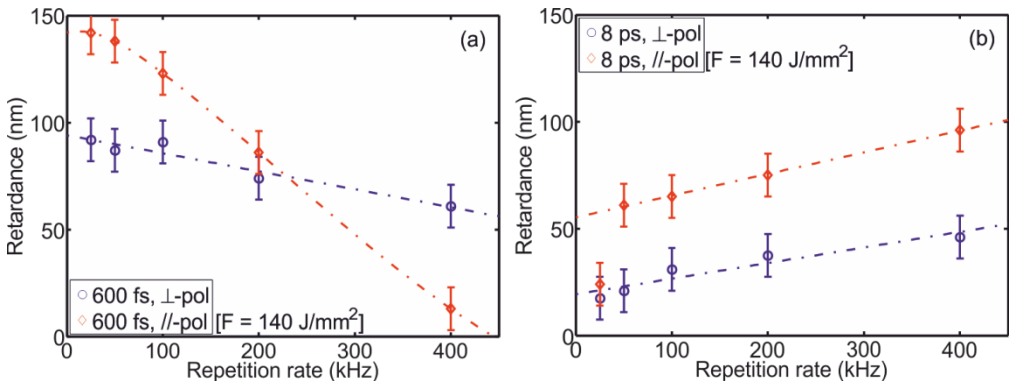

Fig. 4. Dependence of the retardance with the laser repetition rate for (a) 600 fs and (b) 8 ps pulses at fixed net fluence. Dotted-dashed lines are guides for the eye.

Despite the value of the retardance is comparable to what is obtained with fs-lasers, the biggest hurdle to overcome for ps-laser fabricated wave-plates is posed by scattering and by the development of stress regions surrounding the laser tracks resulting in rupture of the glass at high fluences as more and more lines are packed together to raster scan an area of interest. Such a stress build-up is visible in Fig. 1(c) by observing the regions in between lines. A light shade of blue indicates the areas of higher retardance. A model of the laser induced stress distribution allows us to confidently attribute the retardance measured in between lines to stress-induced birefringence. The line-scan in Fig. 1(d) provides evidence that the stress increases as the lines converges.

Finally, we report the observation in laser machining by ps-pulses of the so called “quill effect” whereby laser-matter interaction is shown to be sensitive to the direction of movement of the laser beam [13,26]. A marked sensitivity of the material modification from the direction of writing is observed when 8 ps pulses of 2 μJ pulse energy are focused with a 0.65 NA objective 150 μm below the surface of a silica plate (Fig. 5). Despite we do not have instruments capable of measuring directly the pulse front tilt (PFT) for ps-pulses our findings are compatible with the mechanism originally proposed for fs-pulses. We consider PFT as given by the product of temporal and spatial chirp of the pulse: PFT = AD + GDD × SC where AD is the angular dispersion, GDD is the group-delay dispersion and SC the spatial chirp. The contribution of angular dispersion to the PFT was considered to be negligible due to the absence of astigmatic focal spots in the laser affected zones. The pulses from the picosecond laser were found to be temporally chirped. The spectral bandwidth was measured as 0.26 nm, hence much larger than the transform limited bandwidth of 0.17 nm, giving GDD = 1.1×10^7 fs^2. Such a large value of GDD implies that even a small SC at the resolution limit of our optical spectrum analyzer (0.05 nm) would produce PFT of about 900 fs/mm for a 1 mm diameter collimated beam. For comparison, in fs-laser irradiation of glass writing anisotropy is observed with PFT of the order of 1.8 fs/mm before the focusing lens.

#174210 - $15.00 USD Received 13 Aug 2012; revised 27 Sep 2012; accepted 8 Oct 2012; published 11 Feb 2013

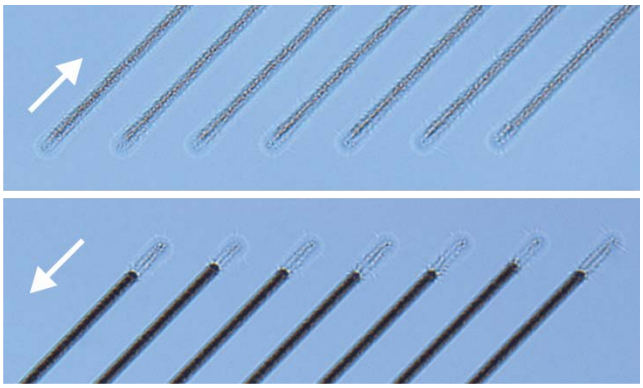

Fig. 5. Microscope bright field images of line structures written in opposite directions using 8 ps pulses. The arrows indicate the direction of writing. The separation between lines is 50 μm. In the top image the damage is uniform along the whole length of the structure. In the bottom image we observe nano-gratings formation (dark lines). Experimental conditions: λ = 1064 nm, NA = 0.65, τ = 8 ps, E_p = 2 μJ, *f* = 200 kHz, *v* = 200 μm/s.

3.2 Assessment of ps-lasers for micro-machining by chemical etching of laser exposed areas

The etching rate of fs-laser irradiated regions has been shown to depend upon the stress and densification in the glass in the low fluence regime and by the nanogratings' orientation in the high fluence regime [9,27]. Hence, the formation of nanogratings by 8 ps-pulses and the concurrent build-up of stress in the regions surrounding the laser tracks will have an impact on the two-step machining by laser irradiation and chemical etching. We looked at aspects that concern the quality of the etched surface, the correlation between etched regions and the light intensity distribution, and finally the etching rate.

The quality of the etched surface is assessed by the SEM imaging of the micro-channel openings (Fig. 6). Although this method cannot provide quantitative information about the wall roughness, it is evident that the channels irradiated by 8 ps laser pulses present an irregular surface. In the irradiated channels etchant penetration produces deep trenches extending beyond the laser affected zones as a result of the formation of either micro-cracks or regions of stress concentration. The lack of correlation between laser intensity profile and etched contour in the picosecond laser two-step machining is a general feature which bears as a consequence our inability to predict the outcome of the etching process from the known applied intensity distribution, ultimately preventing precision micro-machining (Fig. 6). In contrast, femtosecond laser two-steps machining benefits from a very reproducible and reliable process which is known to be primarily driven by the deposited net fluence [28]. This is noticeable in Fig. 7 where each column refers to channels fabricated with the same net fluence but at different laser repetition rate and writing speed. In each column the shape of the aperture of the femtosecond written micro-channels is remarkably similar. This is true even for the lowest fluences where the nanogratings are not fully formed as the number of pulses is below 100. The same cannot be said for two-step machining with 8 ps pulses for which the rate at which the energy is deposited into the silica matrix is shown to play a role (Fig. 6). In fact the size of the micro-channel also grows as the repetition is increased indicating the detrimental effect of heat accumulation and/or pressure build up.

#174210 - $15.00 USD Received 13 Aug 2012; revised 27 Sep 2012; accepted 8 Oct 2012; published 11 Feb 2013

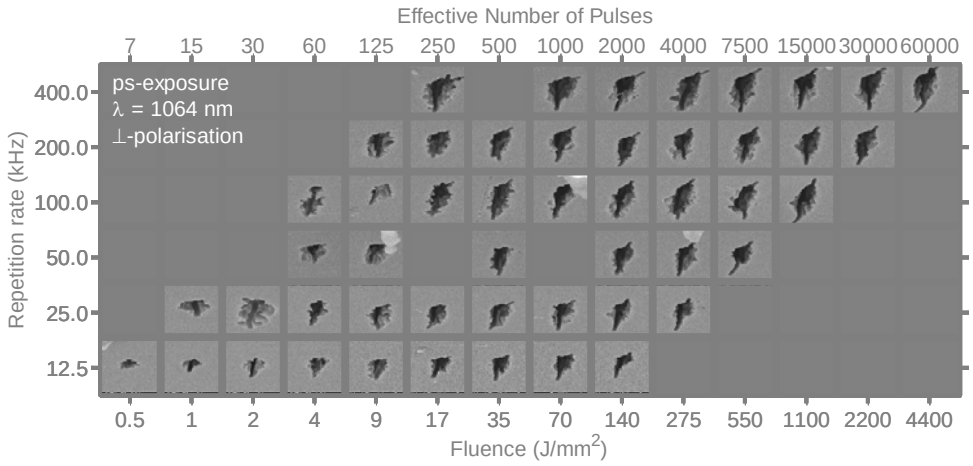

Fig. 6. SEM images of the opening of the etched micro-channels produced by 8-ps laser irradiation followed by 2.5% HF etching for 80 min. E_p = 0.8 μJ, NA = 0.5. Each SEM image is 18.6 μm wide. The writing speed ranged from 25 μm/s to 6400 μm/s.

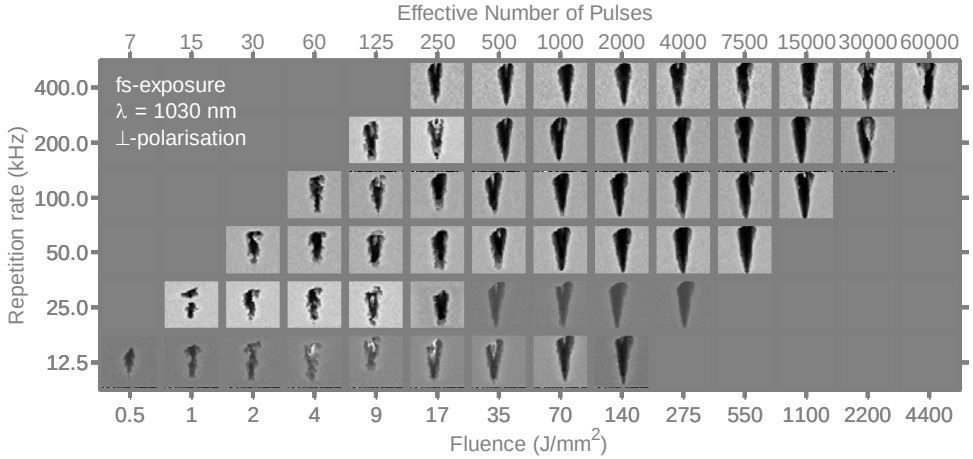

Fig. 7. SEM images of the opening of the etched micro-channels produced by 600-fs laser irradiation followed by 2.5% HF etching for 80 min. E_p = 0.8 μJ, NA = 0.5. Each SEM image is 18.6 μm wide. The writing speed ranged from 25 μm/s to 6400 μm/s

Ultimately, it is the etching rate that defines the aspect-ratio of the structures that can be fabricated by the two-step laser machining (i.e. the higher is the etching rate contrast between pristine and laser-affected zones, the higher is the aspect ratio). Despite the stress region surrounding the laser tracks and the presence of nanogratings, picosecond pulses do not give significant advantage for two-step machining over shorter pulses as the etching rate attains the same maximum value of 2 ± 0.5 μm/min in both ps- and fs- laser irradiated tracks (Fig. 8). However, the dependence of the length of the micro-channel with the net fluence after 80 minutes etching reveals a very different behavior for 8 ps and 600 fs (Fig. 8). In the ps-regime, etched lengths of about 120-150 μm are obtained in the whole range of fluences explored in this study (0.5– 4500 J/mm^2), irrespective of the polarization direction of the writing beam. The same behavior and etched length are obtained also for the etching of laser tracks written at 532 nm. Conversely the etching of channels fabricated by fs-laser pulses presents a far richer dynamic as the fluence is increased with the fastest etching occurring in the low net fluence regime at ~10 J/mm^2 and in the high net fluence regime (~103 J/mm^2).

#174210 - $15.00 USD Received 13 Aug 2012; revised 27 Sep 2012; accepted 8 Oct 2012; published 11 Feb 2013

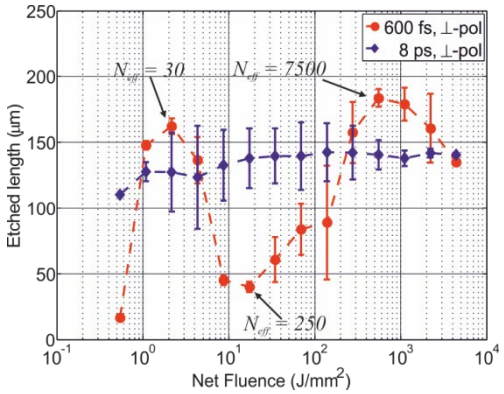

Fig. 8. Comparison of the length of the micro-channel obtained in silica processed by fs- and ps-laser after 80 min in 2.5% HF bath. Each data point in the plot is the average of the etched length of channels exposed at the same net fluence and the error bars give the corresponding standard deviation. Hence, a small error bar indicates that the etched length has little dependence on laser frequency and scanning speed.

The faster etching rate observed in ultra-short pulse laser irradiated silica glass as compared to pristine glass has been ascribed to the structural modification of the material [8], to densification [9] or to the presence of nano-cracks within nanogratings [29]. To distinguish the contributions of nanogratings to the etching process at different fluence regimes, we looked at correlations between the laser induced birefringence (Fig. 3) and the corresponding length of the etched channels (Fig. 8).

In the picosecond regime, the etching rate appears to be constant with the net fluence (Fig. 8). No obvious correlation between birefringence and etching rate is noted by comparison with the retardance measured in Fig. 3.

In the fs-regime the etching rate presents two maxima, one in the low net fluence regime (~10 J/mm^2) and the second in the high net fluence regime (~103 J/mm^2). The trend observed at low fluence was first reported in a previous work carried out at lower pulse energy (0.3 μJ) and in a limited net fluence range [28]. Based on this trend we recognize 4 separate net-fluence regimes. 1) For $N_{eff} < 30$ nanogratings are not formed. However, this is not a type I modification owing to the relatively long pulse duration (600 fs). We confirmed it by measuring a negative average refractive index change by digital holographic microscopy. This regime corresponds to the initial phases prior to the formation of nanogratings. An illustration of this regime is provided by Richter *et al.* and it consists of a chaotic structure with damages randomly positioned in the focal volume [18]. We suppose that in such regime densification occurs within each damage point with consequent onset of a tensile stress. As more and more pulses are accumulated the stress increases explaining the initial rise in the etching rate. Finally, since the damage areas are randomly positioned within the focal volume no effect of the polarization orientation is to be expected in this region. 2) For $30 < N_{eff} < 250$ nanogratings are still not completely formed as evidenced from the birefringence measurements showing that the retardance has not reached its plateau yet. The work by Richter highlights that as the number of pulses increases the glass may start to rupture. The consequence is relaxation of the tensile stress and reduction of the etching rate. 3) As the effective pulse number reaches values $200 < N_{eff} < 7500$, the nanogratings are organized in a well-defined periodic structure. As the net fluence increases, compressive stress develops in the regions surrounding the laser track favoring the etching process. 4) Eventually, for $N_{eff} > 7500$ the glass cannot cope with the increasing pressure and cracks releasing the accumulated stress.

#174210 - $15.00 USD Received 13 Aug 2012; revised 27 Sep 2012; accepted 8 Oct 2012; published 11 Feb 2013

4. Conclusions

In this work we have assessed the suitability of ps-lasers for bulk machining of fused silica relative to two main applications: the fabrication of embedded waveplates and micro-machining by laser irradiation and subsequent chemical etching. Despite pulses shorter than 10 ps - therefore below the limit for strong collateral damage in fused silica glass - were employed the insurgence of a stress field surrounding the laser affected region was observed. Such stress field severely impairs the machining of either waveplates or micro-fluidic/opto-mechatronic devices. In fact, raster scanning of adjacent lines almost inevitably results in deep cracks in the sample and strong light scattering intolerably reduces light transmission through the optical elements. While these effects are not an issue for surface ablation, for which ps-laser are widely used, they make this class of lasers unsuitable for bulk machining of silica glass.

The observation of self-assembled nano-grating and of the change of material modification with the direction of writing by ps-pulses is reported for the first time. The orientation and the period of the nanoplanes are as obtained with fs-pulses. However, the retardance associated with the laser-induced form-birefringence is observed to increase with the laser repetition rate in contrast to femtosecond pulses of the same energy. Picosecond pulses having 10-100 times lower peak intensity than femtosecond pulses are more susceptible to the presence of defects state for the creation of seed electrons. It is suggested that the formation of nanogratings is mediated by defects such as the 2.0 eV excited state of the NBOHCs whose concentration decays on a time scale comparable to the inter-pulse intervals.

Appendix

Self-focusing of a collimated Gaussian beam occurs when the input peak power P_{in} exceeds the critical thresholds P_{cr}. In such a situation the Kerr nonlinearity continuously dominates over the transverse diffraction. The scenario is altered when the beam is tightly focused by a lens. The scope of this appendix is the derivation of an analytical expression that discriminates between a self-focusing dominated regime from the regime where focusing is dominated by the lens so that role of the Kerr nonlinearity maybe neglected.

The propagation length of the self-focusing beam until collapse, L_c, is approximated by the Dawes and Marburger semi-empirical formula [14]:

$$L_c = \frac{0.367 L_{DF}}{\sqrt{\left[\left(\frac{P_{in}}{P_{cr}}\right)^{\frac{1}{2}} - 0.852\right]^2 - 0.0219}}, \tag{1}$$

where L_{DF} is the Rayleigh range of the “collimated” beam,

$$L_{DF} = \frac{k_0 w_0^2}{2} = \frac{\pi n_0 w_0^2}{\lambda} \tag{2}$$

with w_0 and n_0 being the beam waist and the refractive index of air respectively.

Let’s assume that a Gaussian beam is focused by a lens into the bulk of a glass plate of refractive index n (Fig. 9). In the case of a convergent beam the position of the collapse $L_{c,f}$ moves before the linear focus of the lens according to [14]: $1/L_{c,f} = 1/L_c + 1/f$ where f denotes the focal length. Two regimes maybe distinguished:

I. for tight focusing ($f << L_c$) $\rightarrow 1/L_{c,f} \approx 1/f$

II. for loose focusing ($f >> L_c$) $\rightarrow 1/L_{c,f} \approx 1/L_c$.

In regime I lens focusing dominates whereas self-focusing dominates in regime II. The boundary between the two regimes is determined according to:

#174210 - $15.00 USD Received 13 Aug 2012; revised 27 Sep 2012; accepted 8 Oct 2012; published 11 Feb 2013

$$\frac{1}{f} = \frac{1}{L_c} \tag{3}$$

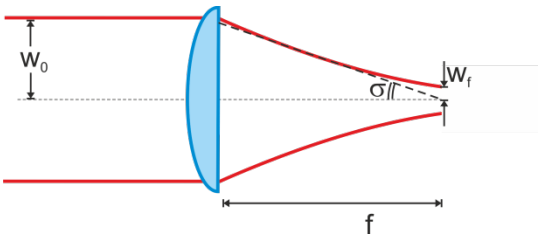

Fig. 9. Schematic of lens focusing and definition of parameters defined in the text.

Let's substitute the expression of L_c from Eq. (1) into Eq. (3). It follows:

$$\sqrt{\frac{P_{in}}{P_{cr}}} = 0.852 + \sqrt{0.0219 + 0.367^2 \left(\frac{L_{DF}}{f}\right)^2} \tag{4}$$

In practice the above relationship is more useful if expressed as a function of the lens numerical aperture (NA) and of the spot size of the collimated beam before the lens w_0.

The numerical aperture is given by:

$$NA = n \sin\sigma = n \frac{t}{\sqrt{1+t^2}} \tag{5}$$

Using trigonometric identities and the expression for the waist at the focus of a Gaussian beam we obtain:

$$t = \tan\sigma = \frac{w_0}{f} \rightarrow t^2 = \left(\frac{w_0}{f}\right)^2 = \frac{w_f^2}{f^2}\left[1 + \left(\frac{\lambda f}{n\pi w_f^2}\right)^2\right], \tag{6}$$

where w_f is the beam waist at the focus. Substitution of the above relationship into Eq. (5) leads to:

$$NA = n \sqrt{\frac{1 + \left(\frac{L_{DF}}{f}\right)^2}{\frac{(kw_0)^2}{4} + \left(\frac{L_{DF}}{f}\right)^2 + 1}} \tag{7}$$

By extracting the term (L_{DF}/f) and substituting into Eq. (4), the following expression is obtained:

$$\sqrt{\frac{P_{in}}{P_{cr}}} = 0.852 + \sqrt{0.0219 + 0.367^2 \frac{\left(\frac{kw_0}{4}\right)^2 - \left(\frac{n}{NA}\right)^2 + 1}{\left(\frac{n}{NA}\right)^2 - 1}} \tag{8}$$

The above equation represents the boundary between the lens-focusing dominated regime and the self-focused dominated regime. Close to the boundary obtained for a given w_o both self-focusing and lens focusing play a role. The calculation does not account for plasma generation. Additionally, it should be noted that the Marburger formula loses its validity for extremely high powers ($P_{in} > 100\ P_{cr}$).

#174210 - $15.00 USD Received 13 Aug 2012; revised 27 Sep 2012; accepted 8 Oct 2012; published 11 Feb 2013

Acknowledgments

This work is supported by the European Commission through the Seventh Framework program. Femtoprint (www.femtoprint.eu), NMP, project no 26010. Prof. N. Bulgakova, B. Poumellec, S. Aktürk and L. Skuja are acknowledged for the insightful discussions. Dr. C. Corbari is in debt with Dr Matthieu Lancry for taking the SEM image of the nanogratings in Fig. 3.

#174210 - $15.00 USD Received 13 Aug 2012; revised 27 Sep 2012; accepted 8 Oct 2012; published 11 Feb 2013